Structural and optical characteristics of silicon nanowires prepared by the Ag-assisted chemical etching method

AHLEM ROUIS[1],*, **NEILA HIZEM**[1], **MOHAMED HASSEN**[2], **CHOHDI AMRI**[3] and **ADEL KALBOUSSI**[1]

[1]Laboratory of Microelectronics and Instrumentation (LR13ES12), Faculty of Science of Monastir, Avenue of Environment, University of Monastir, 5019 Monastir, Tunisia
[2]Higher Institute of Applied Sciences and Technology of Sousse, Taffala City (Ibn Khaldun), 4003 Sousse, Tunisia
[3]Faculty of Science of Bizerte, University of Carthage, 7021 Zarzouna, Tunisia
*Author for correspondence (rouisahlem@gmail.com)

Abstract. In order to improve photovoltaic efficiency, researches have been carried out on silicon nanowires (SiNWs). In this article, we report a comparative study between silicon substrate (Si) and SiNWs developed by a metal-assisted chemical etching (Ag) method at different etching times (25, 10 and 5 min). Scanning electron microscopy (SEM), transmission electron microscopy and X-ray diffraction were used to collect the morphological and structural information on the SiNWs. Raman spectroscopy shows that the intensity of the nanowires is 4 to 10 times higher than that of the substrate, and increases with increase in etching time. The total reflectance of SiNWs reduced to less than 5% over the entire visible range. The low reflectance and zero transmittance of SiNWs lead to higher absorbance in the visible wavelength range. The SiNW-etched nanowire structure (25 min) works best for capturing light, we believe that having longer nanowires improves the optical working of the nanostructures and may be a potential candidate for high efficiency photovoltaic solar cells and other optic devices.

Keywords. SiNWs; SEM; Raman; total reflectance; transmittance; absorption.

1. Introduction

Semiconducting nanowires have become the subject of intensive research in recent years. Hence, a large amount of research has been focused on the utilization of nanowires in a wide range of applications [1,2], such as photodetectors [3], light emitting diodes [4] and solar cells [5,6].

Nanowires characterized by their high aspect ratio, i.e., length to diameter ratio have another interesting property for the grown silicon nanowires (SiNWs) showing wider direct bandgaps when decreasing the diameter and increasing the length. This property triggers the use of SiNWs in optoelectronic devices. Indeed heterojunction solar cells offer an advantage of using combinations of various semiconductors with different bandgaps covering different portions of the solar spectrum. Recently, the antireflective nature of SiNWs, revealed by their black colour and dull appearance, has drawn attention since one of the major energy loss mechanisms of solar cells is optical reflection; utilization of these nanostructures in solar cells may eliminate the need for antireflective coatings [7]. In addition to the photonic and nanoelectronic applications, structures formed of SiNWs could play an important role in the development of innovative 3rd generation photovoltaic cells, allowing achieving conversion efficiencies much higher than those current cells (31%).

However, the optical properties of nanowires depend on their manufacture, because it is of great importance to control their growth and structure. Various methods using top–down or bottom–up approaches have been reported [1,8,9]. Among these methods, metal-assisted chemical etching provides a simple and low-cost approach that enables the fabrication of large-area of nanowires with uniform and controllable height [10]. Since then, many researchers have employed similar methods to fabricate SiNWs arrays using various etching solution systems, like HF/AgNO$_3$ or HF/H$_2$O$_2$/AgNO$_3$ [11,12].

Due to its simplicity and low expensiveness, the Ag-assisted chemical etching method (Ag-ACE) is chosen in this study to elaborate SiNWs. In order to observe structural properties, SEM and XRD have been done showing well-aligned SiNWs growth on a silicon (Si) substrate. The optical properties have been studied by analysing the transmittance, the total reflectance, the absorption and the Raman spectrum.

2. Experimental

Silver (Ag) is chosen as the metal for the growth of SiNWs by the metal-assisted chemical (MACE) method. The substrate used is Czochralski (Cz) solar grade, (100) oriented, p-type boron-doped Si wafers, having a resistivity of 14–25 Ω cm and a thickness of 450 µm. The growth process of SiNWs was elucidated and depicted in figure 1. The wafers were cleaned in a CP4 acid solution (HNO_3: 64%, HF: 16%, CH_3COOH: 20%) for 30 s, then rinsed with deionized water and dried. This step removed approximately 10 to 15 µm of Si from both sides. The samples were immersed in an aqueous solution of 4.8 M HF (40%) and 0.02 M $AgNO_3$ for 60 s to form Ag nanoparticle dendrites films. Then, the Ag-deposited wafers were etched to form the SiNWs in the mixture of 4.8 M of HF (40 wt%) and 0.1 M of H_2O_2 (30 wt%) solution for 5, 10 and 20 min. Subsequently, the as-prepared dark-brown sample was immersed in concentrated nitric acid (HNO_3) for 5 min to remove silver particles, rinsed with deionized water and dried. As the etching proceeds, the SiNWs layer is formed on both sides of the p-Si substrate [13]. Roughened samples are different from the etching time of the nanowires: 5, 10 and 25 min. The growth rate of SiNWs is found to be dependent not linearly on the etching time; the estimated lengths are 2.5, 5 and 12.5 µm, respectively [14]. These samples are compared to a reference (Si-Ref) where the base p-Si substrate was not SiNWs-treated neither annealed.

3. Results and discussion

The scanning electron microscope (SEM, HITACHI 4800) was employed for the surface morphology study; the spectra were measured at normal incidence. Figure 2a and b displays top-view SEM images of the resulting SiNWs. We can clearly see in figure 2a that the SiNWs are distributed almost uniformly over the surface of a Si wafer. The tips of the SiNWs were partially connected to form an open cell-like structure in relation to the etching time. A similar texture has been reported in previous studies [15,16]. Figure 2b shows that the SiNWs are linked to each other to form bundles. This phenomenon is probably due to the attraction of Van der Waals between nanowires and accentuated when the SiNWs are exceeding one micron [17,18]. Furthermore, the nanowires come together to form a diameter of several nanometres. These congregated bundles are uniformly distributed on the sample and confirmed
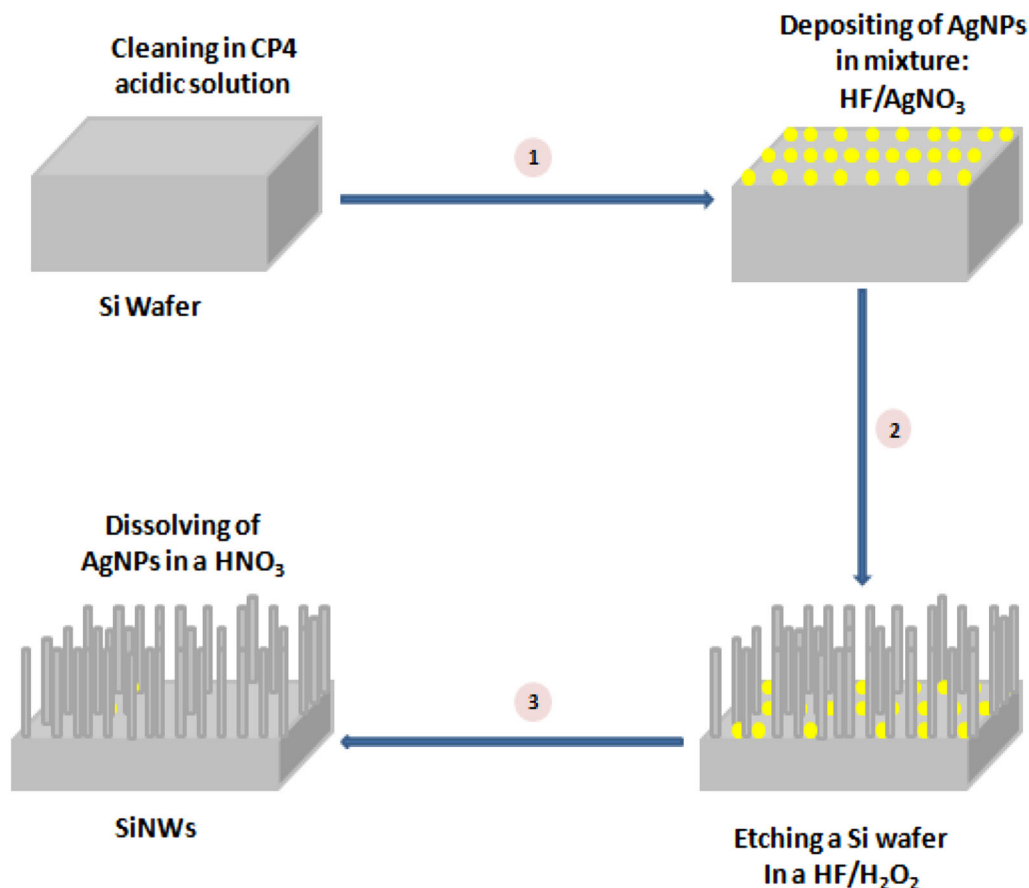

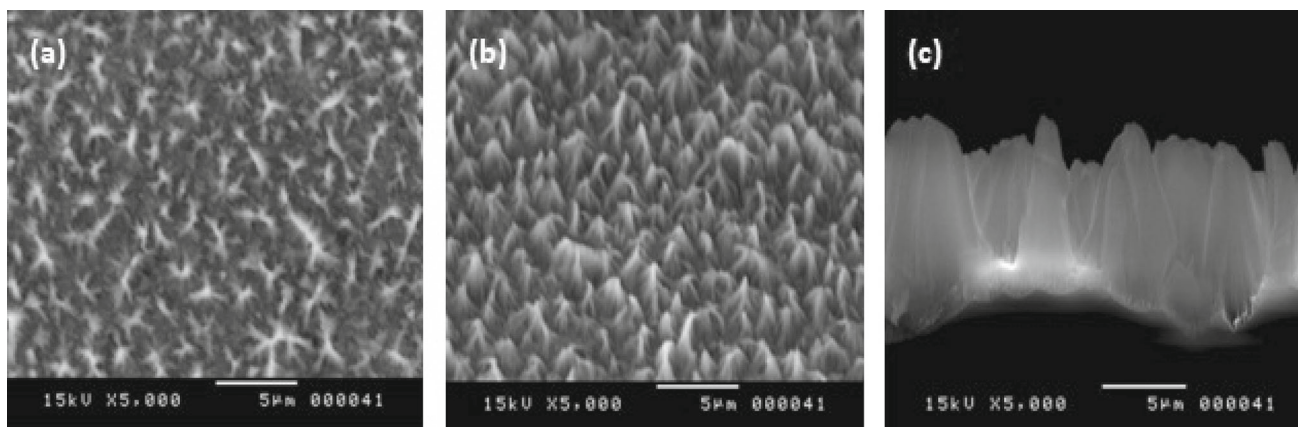**Figure 1.** Schematic illustration for preparation of silicon nanowires by Ag-assisted chemical etching method.

Figure 2. Top view: (**a**) cell-like structure, (**b**) congregated bundles and (**c**) cross-section SEM images of the SiNWs.
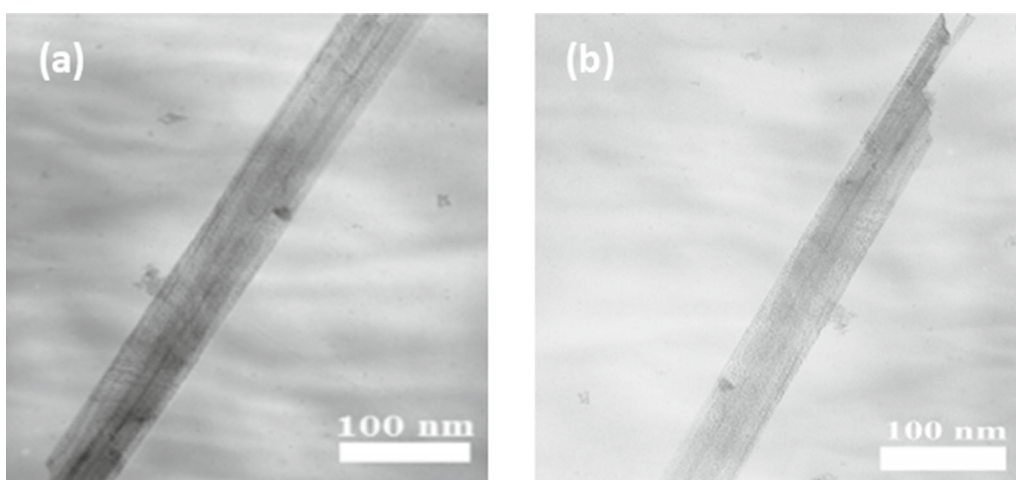

Figure 3. TEM images of individual etched SiNW during (**a**) 5 and (**b**) 25 min, respectively.

from the cross-sectional SEM view shown in figure 2c. This figure shows a well-aligned SiNWs array in the vertical direction. According to the transmission electron microscopy (TEM) images displayed in figure 3a and b, the synthesized SiNWs have a constant diameter almost 100 nm and the estimated lengths are 2.5 and 12.5 μm, respectively.

An X-ray diffractometer (X'pert PRO XRD PW 3040) and Cu kα ($\lambda = 1573$ Å) were used to analyse the structure of the SiNWs. Figure 4 illustrates the relationship between the intensity of SiNWs manufactured at room temperature with different etching times as a function of 2θ. As can be seen from this figure, a unique sharp peak at 70° is observed for all the samples, this suggests high-quality crystalline nanowires [19]. The most crystal structure of the Si is preserved on SiNWs after MACE processing, suggesting that the unique photoelectrochemical properties of the Si is inherited by the SiNWs [20]. On the other hand, the peaks in the same range of diffraction angles are no longer distinguishable, indicating that the SiNWs deposited on the Si substrate are probably largely amorphous.

To verify the optical properties of nanowires on the Si surface, the Raman spectra were recorded in a backscatter
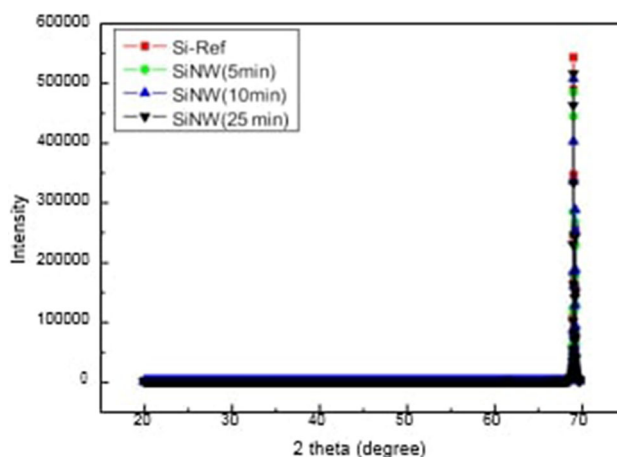

Figure 4. XRD result of SiNWs developed by MACE method.

geometry using Jobin Horiba (T64000 triple monochromator) micro-Raman spectrometer in a back scattering geometry. The Raman scattering modes were excited by an argon ion laser (514.5 nm, 30 mW). Figure 5 shows the typical spectra of the Raman scattering of SiNWs and Si substrate
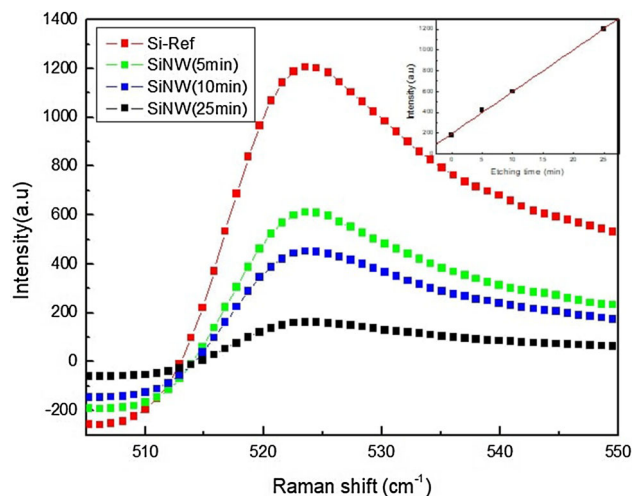
Figure 5. Raman spectra of SiNWs and Si substrate (Si-Ref) excited by an argon ion laser (514.5 nm, 30 mW) at room temperature, and the inset shows dependence of the Raman intensity on the etching time of SiNWs (dashed red curve corresponds to a fit by the linear function).

Figure 6. Total reflectance spectra of Si-Ref and SiNWs etched at different durations.

for comparison. The scattered light intensity shows only a broad maximum (peak at 523 cm^{-1}) and is otherwise featureless. The position and shape of the Raman peak for SiNWs are similar to the Si-Ref. This is certainly due to a large diameter of nanowires, which is far from the quantum confinement regime. However, the intensity is 4 to 10 times higher for nanowires than that for the Si substrate, and increases considerably by increasing the etching time. The SiNWs intensity increase linearly with etching time up to 25 min as was also pointed in the inset of figure 5. The possible reasons behind this increase may be ascribed to the fact that etching was given more time to proceed and the solution had enough oxidizing species. Therefore, Raman scattering intensity depends on the length of SiNWs. The same results were also observed for the SiNWs produced by the MACE method [21]. This increased intensity is due to the strong light scattering and the partial light localization in an inhomogeneous optical medium [22]. Another interpretation of Raman scattering in SiNWs arrays is based on taking into account the incident electromagnetic radiation resonance of each SiNWs. While both interpretations are possible, it can be deduced that the high Raman intensity indicates a high crystalline quality of the nanowires.

By analysing the total reflection spectrum of SiNWs, the effect of light localization was studied in more detail. It has been shown that the reflection of nanowires covered Si surface depends mainly on the nanowire length, diameter and density. Indeed, nanowires length of several μm was found necessary to reduce the reflectivity to less than 2% in a much smaller portion of the wavelength range [23]. Figure 6 shows the total reflection spectrum of a crystalline Si substrate (Si-Ref) and the SiNWs samples. The reflectance of Si-Ref shows the typical behaviour expected for Si with a maximum of 80–70% in the ultraviolet (UV) and
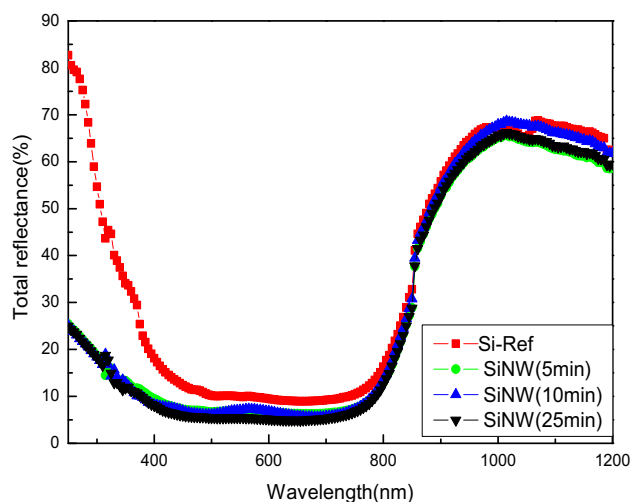
near-infrared (IR) regions, and a minimum of 10% in the visible spectrum region.

However, SiNWs sample showed a significant reduction in reflectance to 25% in the UV range and a reduction of 5% in the visible spectral range in comparison to the Si-Ref. The reflectance of all samples is increased to 70% for a wavelength greater than 800 nm. It can be seen that the modification of the surface morphology of the Si substrate forming the SiNWs successfully reduced the loss of reflection of the incident radiation in the visible spectral range from 10% to less than 5%. This can be explained by the strong scattering and absorption of light, which leads to the partial localization of the excitation light in the SiNWs. As readily seen in the figure, all the reflectance values of SiNW arrays at different etching times with various lengths are almost close, owing to the same diameter of nanowires and the tapered NWs structure [19]. Therefore, SiNWs produced using inexpensive chemical etching result in reduced optical losses This property meets the requirements for applying SiNWs in photosensitive devices capable of effectively detecting incident light. In the visible spectral range, samples containing SiNWs would be similar to 'black silicon' and could be used as anti-reflective coatings in photovoltaic applications [21,22].

Optical transmission was also carried out in SiNWs, which is ready to understand the absorption of light in nanostructures. A UV/VIS/NIR Spectrometer Perkin-Elmer Lambda 950 equipped with an integrating sphere was used to measure the total transmission in the wavelength range from 300 to 1200 nm. Figure 7 illustrates a comparison of the optical transmittance of SiNWs with different etching times and the reference sample (Si-Ref) measured at 300 K. The optical transmittance spectra of SiNWs show several important points. First, all these samples present a strong
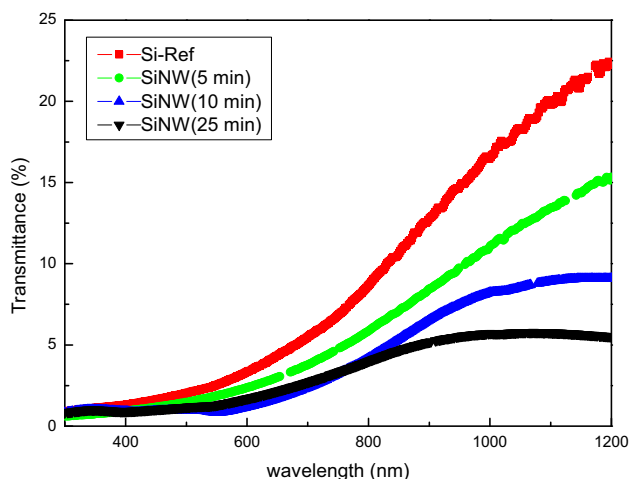
Figure 7. Optical transmittance spectra of SiNWs and Si-Ref at room temperature.
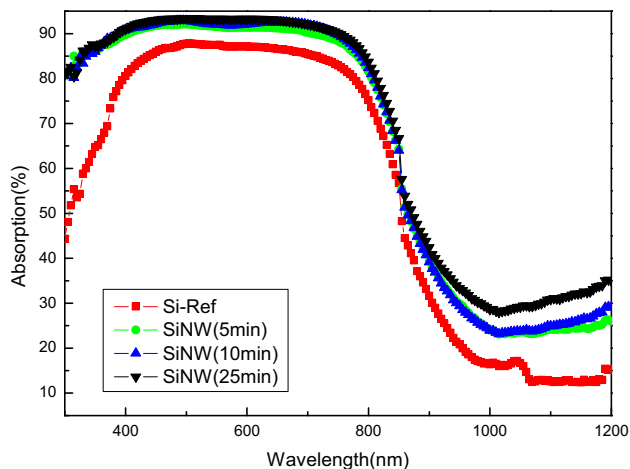

Figure 8. Optical absorption spectrum of SiNWs etched at different times.

dependence of optical transmittance on the spectral wavelength; very opaque to incident short-wavelength light with wavelengths below ∼400 nm, while relatively transparent in the long-wavelength spectral region of 800–1200 nm. Secondly, the transmittance of the reference sample is higher than that of SiNWs at wavelength >800 nm and decreases with increase in the etching time. Consequently, the reduction of transmittance of SiNWs indicates that there is a strong absorption in the nanowire layer, for example, due to a large light trapping [24]. In fact, the light trapping mechanism formed by the array of SiNWs of high aspect ratio will significantly reduce the intensity of transmittance. Therefore, with its low transmittance, SiNWs encourages its use as a surface texture microstructure, as an anti-reflective coating on top of a processed solar cell [6,25].

From the reflectance and transmission measurements, we have calculated the absorption spectra as shown in figure 8. As expected, the absorbance of SiNWs rises with the increase of etching time and reaches 100% for low

wavelength range. The etched nanowire structure SiNW (25 min) performs the best in capturing light in comparison with Si-Ref sample, especially at wavelength lower than 800 nm. Indeed greater quantum confinement of photon occurs and for this reason, high absorption achieved. This inspection facilitates that the synthesized SiNWs by MACE method could be a potential contender for efficient photovoltaic solar cells.

4. Conclusion

In summary, we have reported a high-quality SiNWs produced by MACE method at different etching times. From SEM, TEM and XRD analysis, we noticed that the etching preserved the formation of vertical and aligned SiNW arrays, which followed the direction of the Si wafer substrate. Increasing etching duration leads to a longer length without affecting the wire diameter, which remains almost constant nearly 100 nm. Compared to the Si-Ref, the formed SiNWs have a considerably increased Raman scattering intensity. The relative increase in the intensity of the Raman signal with the increase in the etching time is interpreted as proof of the position of the light due to the multiple scattering. The average reflectance of SiNWs is less than 5% within a range of wavelengths between 400 and 800 nm. The reflectance values (R) are much smaller than those of Si substrate (that shows an R of more than 10%). Therefore, these nanowire structures can be used for anti-reflection applications in a wide solar spectral range. The low reflectance observed is correlated with the weak transmittance in the visible range. Indeed the light transmissions are opaque (high absorption) at short wavelength (<400 nm) and relatively transparent in the long wavelength spectral region (>800 nm). Moreover, the transmission of the SiNWs structures was observed to be lower than that of a Si-Ref and decreases when the etching time increases. The low reflectance and zero transmittance of SiNW lead to higher absorbance compared to the Si-Ref sample in the visible wavelength range. Furthermore, the SiNW-etched nanowire structure (25 min) works best for capturing light, which leads us to believe that having longer nanowires improves the optical working of the nanostructures. These optical phenomena sell proposals for the realization of efficient solar cells based on engraved SiNWs manufactured by a simple chemical method on a large scale.

References

[1] Hutagalung S D, Fadhali M M, Areshi R A and Tan F D 2017 *Nanoscale Res. Lett.* **12** 425

[2] Yu P, Wu J, Liu S, Xiong J, Jagadish C and Wang Z M 2016 *Nano Today* **11** 704

[3] Bae J, Kim H, Zhang X M, Dang C H, Zhang Y, Choi Y J *et al* 2010 *Nanotechnology* **21** 095502

[4] Qian F, Gradecak S, Li Y, Wen C Y and Lieber C M 2005 *Nano Lett.* **5** 11

[5] Hu L and Chen G 2007 *Nano Lett.* **7** 3249

[6] Sivakov V, Andrä G, Gawlik A, Berger A, Plentz J, Falk F *et al* 2009 *Nano Lett.* **9** 1549

[7] Srivastava S K, Kumar D, Singh P K, Kar M, Kumar V and Husain M 2010 *Sol. Energy Mater. Sol. Cells* **94** 1506

[8] Za'bah N F, Kwa K S, Bowen L, Mendis B and O'Neill A 2012 *J. Appl. Phys.* **112** 024309

[9] Ramanujam J, Shiri D and Verma A 2011 *Mater. Express.* **1** 105

[10] Wang W, Li D, Tian M, Lee Y C and Yang R 2012 *Appl. Surf. Sci.* **258** 8649

[11] Zhang C, Li S, Ma W, Ding Z, Wan X, Yang J *et al* 2017 *J. Mater. Sci.: Mater. Electron.* **28** 8510

[12] Boarino L, Imbraguglio D, Enrico E, De Leo N, Celegato F, Tiberto P *et al* 2011 *Phys. Status Solidi A* **208** 1412

[13] Amri C, Ouertani R, Hamdi A and Ezzaouia H 2016 *Superlattices Microstruct.* **91** 278

[14] Amri C, Ouertani R, Hamdi A and Ezzaouia H 2017 *Mater. Sci. Semicond. Process.* **63** 176

[15] Lajvardi M, Eshghi H, Ghazi M E, Izadifard M and Goodarzi A 2015 *Mater. Sci. Semicond. Process.* **40** 556

[16] Canevali C, Alia M, Fanciulli M, Longo M, Ruffo R and Mari C M 2015 *Surf. Coat. Technol.* **280** 37

[17] Qiu T, Wu X L, Shen J C, Ha P C and Chu P K 2006 *Nanotechnology* **17** 5769

[18] Peng K, Lu A, Zhang R and Lee S T 2008 *Adv. Funct. Mater.* **18** 3026

[19] Naffeti M, Postigo P A, Chtourou R and Zaïbi M A 2020 *Nanomaterials* **10** 404

[20] Meng H, Fan K, Low J and Yu J 2016 *Dalton Trans.* **45** 13717

[21] Gonchar K A, Zubairova A A, Schleusener A, Osminkina L A and Sivakov V 2016 *Nanoscale Res. Lett.* **11** 357

[22] Gonchar K A, Osminkina L A, Galkin R A, Gongalsky M B, Marshov V S, Timoshenko V Y *et al* 2012 *J. Nanoelectron. Optoelectron.* **7** 602

[23] Ozdemir B, Kulakci M, Turan R and Unalan H E 2011 *Nanotechnology* **22** 155606

[24] Tsakalakos L, Balch J E, Fronheiser J, Shih M Y, LeBoeuf S F, Pietrzykowski M *et al* 2007 *J. Nanophotonics* **1** 013552

[25] Asgar M A, Hasan M, Huq M F and Mahmood Z H 2014 *Int. Nano Lett.* **4** 101